Selectivity of Retinal Photoisomerization in Proteorhodopsin Is Controlled by Aspartic Acid 227†

Eleonora S. Imasheva, Sergei P. Balashov,* Jennifer M. Wang, Andrei K. Dioumaev, and Janos K. Lanyi

Department of Physiology and Biophysics, University of California, Irvine, California 92697

Received September 4, 2003; Revised Manuscript Received November 28, 2003

ABSTRACT: Similarly to bacteriorhodopsin, proteorhodopsin that normally contains all-*trans* and 13-*cis* retinal is transformed at low pH to a species containing 9-*cis* retinal under continuous illumination at $\lambda > 530$ nm. This species, absorbing around 430 nm, returns thermally in tens of minutes to initial pigment and can be reconverted also with blue-light illumination. The yield of the 9-*cis* species is negligibly small at neutral pH but increases manyfold (>100) at acid pH with a pK_a of 2.6. This indicates that protonation of acidic group(s) alters the photoreaction pathway that leads normally to all-*trans* → 13-*cis* isomerization. In the D97N mutant, in which one of the two acidic groups in the vicinity of the retinal Schiff base is not ionizable, the yield of 9-*cis* species at low pH shows a pH dependence similar to that in the wild-type but with a somewhat increased pK_a of 3.3. In contrast to this relatively minor effect, replacement of the other acidic group, Asp227, with Asn results in a remarkable, more than 50-fold, increase in the yield of the light-induced formation of 9-*cis* species in the pH range 4−6. It appears that protonation of Asp227 at low pH is what causes the dramatic increase in the yield of the 9-*cis* species in wild-type proteorhodopsin. We conclude that the photoisomerization pathways in proteorhodopsin to 13-*cis* or 9-*cis* photoproducts are controlled by the charge state of Asp227.

Proteorhodopsins[1] are retinal proteins recently discovered in proteobacteria (*1*−*4*). Similarly to bacteriorhodopsin of the archaea, proteorhodopsin from Monterey Bay is able to make use of the energy of absorbed quanta by transporting protons from the inside to the outside of the cell. At the slightly alkaline pH of ocean water, proteorhodopsin exhibits a photocycle that includes formation of an M intermediate and transient proton uptake followed by release (*1*, *5*). As in bacteriorhodopsin, the photocycle involves all-*trans* → 13-*cis* photoisomerization of the chromophore, transient deprotonation of the Schiff base in the M intermediate coupled to the protonation of the internal proton acceptor Asp97, and thermal reisomerization of the chromophore during the N → PR transition (*5*, *6*). Most of the key residues forming the retinal binding pocket, and particularly those involved in proton transport, are conserved. These include the internal proton acceptor, Asp85 in BR and Asp97 in PR, and the internal proton donor, Asp96 in BR and Glu108 in PR, and also components of a complex counterion to the Schiff base, Arg82 and Asp212 in BR, which are Arg94 and Asp227 in PR. However, the Glu204−Glu194 pair which is a part of the proton release complex in BR (*7*−*9*) is replaced in PR by nonionizable residues (*1*).

At pH below 8 a red shift of the absorption maximum of PR in the unphotolyzed state is correlated with the absence of the M intermediate in the photocycle. Both of these facts were attributed to protonation of Asp97 (*10*). The pK_a of Asp97 (around 7.1−7.6, a value dependent on conditions) is much higher than the pK_a of Asp85 in purple membrane containing bacteriorhodopsin (pK_a = 2.6).

Earlier laser flash-induced kinetic studies (*1*, *5*, *6*, *11*, *12*) provided information on short-lived intermediates of the photochemical cycle of PR. In this study, we investigated the long-lived light-induced species that accumulate in PR and its mutants under continuous illumination at low pH. We found that upon illumination at $\lambda > 530$ nm PR undergoes transformation to a species absorbing at 430 nm. The yield of this species exhibits strong pH dependence, increasing manyfold below pH 3. It can be converted back to PR by blue-light illumination. FTIR spectra indicate that the 430 nm species contains 9-*cis* retinal, and thus it is analogous to the so-called "pink membrane" of bacteriorhodopsin. Light-induced formation of the 9-*cis* species is strongly enhanced in the D227N mutant but not in D97N. These results indicate that when anionic, Asp227 facilitates the all-*trans* → 13-*cis* photoisomerization pathway, and prevents formation of 9-*cis* photoproducts.

MATERIALS AND METHODS

The proteorhodopsin gene used was isolated from uncultivated proteobacteria from Monterey Bay (*1*). The protein is 6xHis-tagged at the C-terminus and the three cysteines it contains (Cys107, Cys156, and Cys175) were replaced with valines (the so-called triple-cysteine mutant, TCM (*10*)) to prevent their oxidation and thereby make the pigment more

† This work was supported by grants from the National Institutes of Health GM29498 (to J.K.L.) and Department of Energy DEFG03-86ER13525 (to J.K.L.).

* To whom correspondence should be addressed. Phone: (949) 824-7783. Fax: (949) 824-8540. E-mail: balashov@uci.edu.

[1] Abbreviations: PR, proteorhodopsin; BR, bacteriorhodopsin; DM, *n*-dodecyl-*β*-D-maltopyranoside; NM, *n*-nonyl-*β*-D-maltopyranoside; OG, *n*-octyl-*β*-D-glucopyranoside; BICINE, *N*,*N*-bis[2-hydroxyethyl]-glycine; CAPS, 3-cyclohexylamino-1-propanesulfonic acid; CHES, 2-[*N*-cyclohexylamino]ethanesulfonic acid; MES, 2-[*N*-morpholino]-ethanesulfonic acid; MOPS, 3-[*N*-morpholino]propanesulfonic acid.

10.1021/bi0355894 CCC: $27.50
Published on Web 01/24/2004

stable upon storage. We will refer to this pseudo-wild-type protein simply as PR, because its properties are similar to those of the wild-type. The protein was expressed in *Escherichia coli* (UT 5600 strain), using the vector kindly provided by J. L. Spudich and E. N. Spudich and following the procedures described in ref *1*. All-*trans*-retinal was added to whole cells (0.1 mL of 100 mM stock ethanol solution to 1 L of culture) during induction of proteo-opsin biosynthesis. To purify the reconstituted pigment, the cells were treated with lysozyme in the presence of DNAase and then passed through a French press. The membranes were solubilized in a detergent (OG) and the pigment was purified on a Ni−NTA Agarose column, as described earlier (*10*). To check whether properties of the pigment are substantially altered by solubilization, we conducted comparative titrations in a wide pH range in several detergents (OG, DM, NM). Because the solubilization of the pigment is more efficient in OG, it was used for initial solubilization of the membranes. However, this detergent substantially increases the pK_a of Asp97 (to 8.2) and at the same time decreases the pK_a of the Schiff base (from >11.5 to less than 10.5). These pK_a's in DM (7.6 and ca. 11.3, Figure 1C,D) were closer to those in membranes (*5*) and purified PR (*6*). For these reasons, DM was chosen as the detergent for all absorption spectra measurements. Substitution of OG with DM was done using an Amicon stirred cell with an Amicon YM30 ultrafiltration disk. The samples contained 0.1% DM, 100 mM NaCl, and six buffers, 5 mM each (BICINE, CAPS, CHES, citric acid, MES, MOPS).

The mutant proteins (D97N and D227N) were expressed in *E. coli* as described earlier (*10*). In each of these mutants, the three cysteines were also replaced as in the TCM mutant.

Absorption spectra were measured using a Shimadzu UV-1601 spectrophotometer. A Cole-Parmer 9741−50 illuminator (150W) in combination with a light guide, bandpath and interference filters were used for actinic illumination. The intensity of actinic light λ > 530 nm in the range 530−650 nm was ca. 15 mW/cm^2. The intensity of the blue (340−500 nm, maximum at 425 nm) light was 2 mW/cm^2.

Light-induced changes in the chromophore isomeric state in proteorhodopsin and bacteriorhodopsin were monitored by FTIR spectroscopy. For measurements on proteorhodopsin, column-purified solubilized (in OG) PR was incorporated into egg-PC liposomes (Avanti # 840051C L-α-phosphatidylcholine) at a 1:5 protein-to-lipid ratio. The liposome formation was induced by decreasing the concentration of OG from 1.3 to 0.17%. The detergent was washed out by two consecutive centrifugations at 250000*g* for 2 h at 4 °C. The suspension of purple membrane or liposomes containing proteorhodopsin was washed from residual traces of Cl^- and placed on CaF_2 windows and air-dried. Humidified films with pH set to the desired value (2.3 for PR, 3.5 for D97N, and 4 for D227N) were obtained by soaking these films first in 5 mM citric acid (2 times for 20 min) and then for additional 20 min in 1 mM citric acid. The films were allowed to dry to the point when the water content was about 100−200 molecules per protein molecule, as estimated from the ratio of amplitudes in the absolute IR absorption spectrum at 1654 cm^{-1} to that at 1547 cm^{-1}, which was approximately 1.2 (for PR).

Light-induced conversions in films were produced by continuous illumination at λ > 530 nm for PR and λ > 630 nm for BR. The light source was a 175 W Cermax xenon lamp (ILC Technology, Sunnyvale, CA), equipped with a 5-mm-diameter liquid light guide. Light intensity was approximately 10−15 mW/cm^2. "Light minus dark" difference spectra were obtained as a difference between steady-state spectrum observed under illumination and spectrum in the dark (before illumination or after relaxation of the photoproducts).

IR data were collected on a Bruker IFS-66/s FTIR spectrometer at 2 cm^{-1} resolution for the 0−1970 cm^{-1} range with the scanning frequency of 180 kHz, resulting in co-adding of 3098 interferograms during each 10-min interval. Contributions to the spectrum from changes in the water vapor content were subtracted.

RESULTS

pH Dependence of Dark (Thermal) Transitions in Solubilized Proteorhodopsin and Its Mutants. Figure 1A,B shows spectral transitions induced by changing the pH. Upon increasing the pH from 5 to 9 a blue shift of the absorption maximum, from 543 to 511 nm, occurs (Figure 1A), caused by deprotonation of Asp97 as shown in an earlier study (*5*). The pH dependence of the absorption changes at the minimum of the difference spectrum (564 nm) can be described by a titration curve with pK_a 7.6 (Figure 1C). An interesting feature of PR is that it does not show the blue shift seen in BR at pH < 2 in the presence of 100 mM chloride due to binding of chloride ion at the vicinity of the Schiff base (the "acid purple species") (*13*−*16*).

At pH > 10.5 deprotonation of the Schiff base takes place, yielding a species that absorbs at 370 nm (Figure 1B). The pK_a of this transformation is 11.3 (Figure 1D). The increase of the absorption at 298 nm (Figure 1B) is from deprotonation of tyrosines, seen also in BR at high pH (*17*).

As described before (*5*), the D97N mutation eliminates the blue shift of the chromophore (data not shown), which is observed in PR upon increasing the pH above 7 (Figure 1A), in agreement with the assignment of this shift to deprotonation of Asp97. Deprotonation of the Schiff base in D97N in the dark occurs with a pK_a, substantially lower than in PR (9.7 versus 11.3, see Figure 1D). The deprotonated chromophore in D97N absorbs at ca. 400 nm.

Mutation of the other aspartic acid residue in the retinal binding site, Asp227, resulted in a pigment with absorption maximum slightly (2−3 nm) blue shifted compared to PR (at pH 3). The mutation affected the pK_a's of the pH-induced transitions in the dark associated with deprotonation of Asp97 and the Schiff base. The blue shift of the absorption maximum from 536 nm at pH 3 to 510 nm at pH 8 exhibits a complex titration. The first transition occurs with a pK_a ca. 4.0 (Figure 1C); it is accompanied by a shift from 536 to 522 nm and characterized by an isosbestic point at 530 nm (data not shown). Another shift, from 522 nm to ca. 510 nm (isosbestic point at 504 nm), occurs with a pK_a of 6.4. The latter pK_a is about 1.2 units lower than the analogous transition in PR, suggesting that, as one might expect from the proximity of the two aspartic acid residues, neutralization of Asp227 results in a decrease in the pK_a of Asp97. The origin of the biphasic titration is not clear. The pK_a of the Schiff base was also decreased, by about 1 unit to 10.5 (Figure 1D). The deprotonated species absorbs at 365 nm.

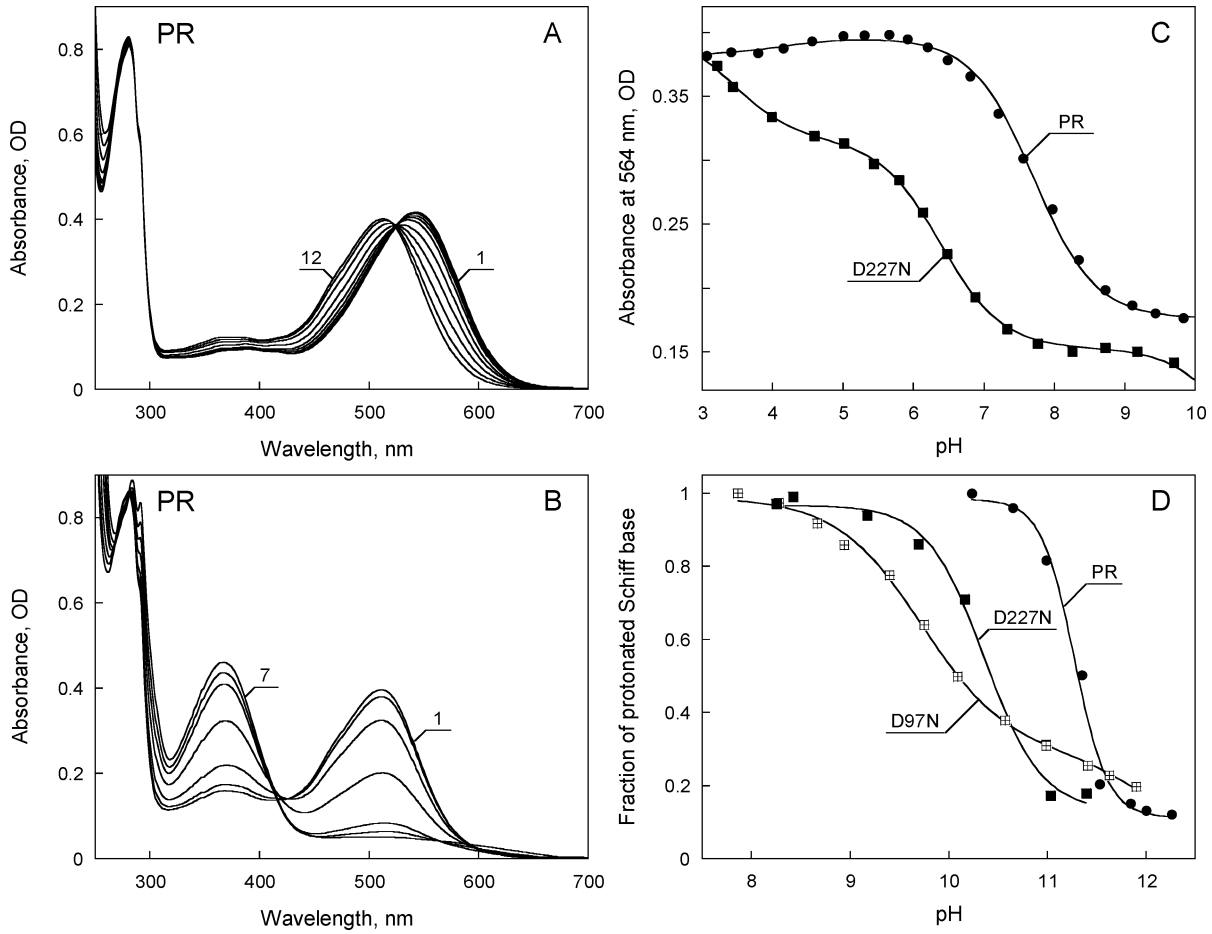

FIGURE 1: pH-dependent spectral transitions in proteorhodopsin (in 0.1% DM, 100 mM NaCl) associated with deprotonation of Asp97 (A, C) and the Schiff base (B, D). (A) Absorption spectra taken upon increasing the pH from 5 to 9 with approximately 0.3 pH units increments (curves 1 and 12, respectively). (B) Absorption spectra of proteorhodopsin upon increasing the pH from 10.2 to 12.3 (curves 1 and 7, respectively). (C) pH dependence of absorption changes at 564 nm for PR (fitted with a titration curve with pK_a 7.6, $n = 1$) and D227N mutant (fitted with two pK_a's, 3.4 and 6.4). (D) pH dependence of absorption changes at the maximum (511 nm for PR and D227N and 536 nm for D97N mutant). Fits of the titration curves, PR, pK_a 11.3, $n = 2.6$; D97N, pK_a's 9.7, and 12.1, $n = 1$; D227N, pK_a 10.4, $n = 1.5$.

Reversible Light-Induced Transformation of Proteorhodopsin under Continuous Illumination. Illumination of PR at pH 6 at moderate light intensity ($\lambda > 530$ nm) for 10 min causes small spectral changes in the sample, but at low pH a large fraction of the pigment is photoconverted to long-lived product. At pH < 4 a species with an absorption maximum around 430 nm is formed (Figure 2A,B). This photoproduct exhibits a very low extinction coefficient compared to initial PR (ca. 2-fold lower). In the dark, the 430 nm species converts partly back to PR with a time constant of about 30 min, and partly to a 370 nm species (Figure 2C,D). Upon blue-light illumination, the 430 nm species nearly completely reconverts to PR.

FTIR Difference Spectra Accompanying Formation of the 430 nm Species in Proteorhodopsin: Comparison with the Pink Membrane of Bacteriorhodopsin. The light-induced reversible transition in proteorhodopsin to the 430 nm species involves a 100-nm blue shift of the absorption maximum and large decrease in extinction. This transition appears similar to those that occur at low pH in bacteriorhodopsin and result in conversion to a 500 nm species (*18*, *19*). The latter was shown to involve isomerization of the chromophore from all-*trans* to 9-*cis* (*18*, *19*) yielding the "pink membrane" (*20*), which was characterized both with resonance Raman (*21*) and FTIR (*22*) vibrational spectroscopy. Figure 3 compares FTIR difference spectra for the light-induced transitions in BR and PR. The strong upshift of the ethylenic stretch bands in Figure 3A (from 1517 to 1545 cm^{-1}) is from the blue-to-pink membrane transition in BR. It is in accord with the earlier-described FTIR (*22*) and resonance Raman lines of ethylenic stretch in the blue membrane at 1518 cm^{-1} (*22*, *23*) and at 1542 cm^{-1} in the pink membrane (*21*). In PR, the analogous reaction upshifts the ethylenic stretch from 1529 to 1553 cm^{-1} (Figure 3B). The shifts of the ethylenic bands of the two proteins to higher frequencies are in agreement with the large blue shifts (90−100 nm) of the absorption maxima in the visible spectral range, which were observed both in water suspensions and humidified films.

The fingerprint region of the FTIR spectrum of the pink membrane lacks the strong positive band of 13-*cis* retinal at 1186−1194 cm^{-1} (characteristic for the K, L, and N intermediates of BR (*24*)), we find a positive band at 1214 cm^{-1} instead (Figure 3A). A prominent band at this frequency was earlier noted in the resonance Raman spectrum of the 9-*cis* species of the pink membrane (*21*). In the FTIR spectrum of the pink membrane the band at 1212 cm^{-1} is present as the main peak in the fingerprint region (*22*). A similar but less intense band is in the resonance Raman

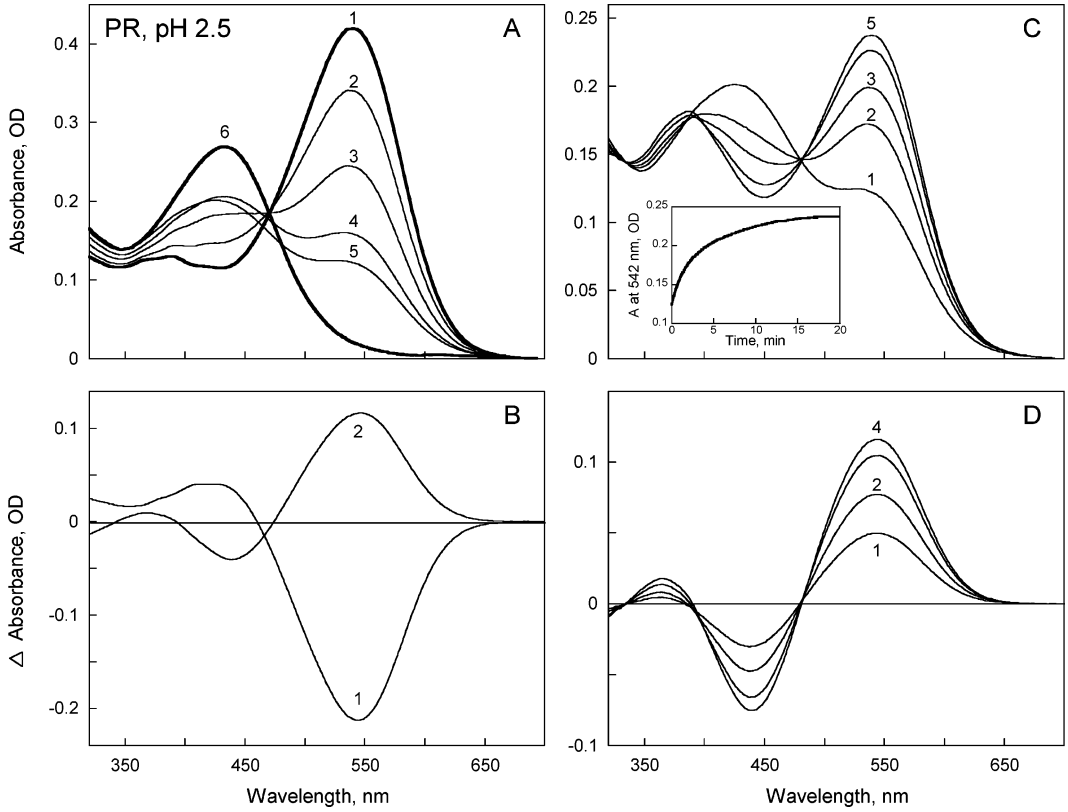

FIGURE 2: (A) Photoconversion of PR to a 430 nm species upon illumination with $\lambda > 530$ nm at pH 2.5: 1, initial spectrum; 2−5, spectra after illumination at >530 nm for 15 s, 45 s, 1.5 min, and 5 min, respectively; 6, spectrum of the 430 nm species obtained as a sum of initial spectrum and the difference spectrum after 45 s illumination multiplied by 2.27. (B) Difference spectra produced by: 1, 5 min illumination at >530 nm; 2, subsequent 5 min illumination at 350−470 nm. (C) Thermal conversion of the 430 nm species back to PR and the 365 nm species: 1, after 5 min illumination at > 530 nm (same as curve 5 in panel A); curves 2−5, after incubation in the dark for 5, 10, 20, and 40 min, respectively. Inset: Kinetics of the 430 nm species to PR thermal conversion at 0−20 min time interval. (D) Difference spectra of thermal transitions shown in panel C.

spectra of *trans*-bacteriorhodopsin as well. The latter was specifically assigned to C_8-C_9 stretch coupled to C_9-CH_3 stretch and $C_{10}-H$ in-plane rock (*25*). However, if the 1214 cm^{-1} band originated from all-*trans* retinal, it would have appeared as a *negative* band, together with the other negative bands from all-*trans* depletion (i.e., at 1252, 1198, and 1167 cm^{-1}). Instead, the FTIR spectrum in Figure 3A contains a strong *positive* band at 1214 cm^{-1}, signaling an increase in intensity of the C_8-C_9, C_9-CH_3, and $C_{10}-H$ contributions upon isomerization of the retinal to the 9-*cis* configuration, as suggested by ref *21*. Importantly, Figure 3B shows that a similar band at 1216 cm^{-1} appears upon illumination of PR, and as in BR there are no positive bands from 13-*cis* retinal. The presence of both positive band at 1216 cm^{-1} and negative bands from all-*trans* (1162, 1197, and 1254 cm^{-1}) and 13-*cis* (1183 and 1234 cm^{-1}) parent chromophores in the FTIR spectrum of PR (Figure 3B) is evidence that the photoconversion at low pH leads to formation of 9-*cis* species not only in BR but in PR also. In PR the 9-*cis* species are formed mainly from all-*trans* and a smaller fraction from 13-*cis* (as indicated by the presence of negative bands at 1183 and 1234 cm^{-1}). The latter could be from 13-*cis*,15-*syn* to all-*trans* reequilibration when the light reaction depletes the all-*trans* population. The photoproducts formed upon illumination of the D97N and D227N mutants at low pH exhibited similar difference spectra, including a positive band at 1218 (in D97N) or 1214 (in D227N) cm^{-1}, which indicate that they are 9-*cis* species (Figure 3C,D).

Strong positive bands at 1651 cm^{-1} for BR and 1658 cm^{-1} for PR in the amide I region indicate substantial conformational changes in the transition to 9-*cis* photoproducts. These phototransformations are accompanied by other specific changes detectable in the infrared, for instance, in the region of the protonated C═O stretch of carboxylic groups. These will be described in a separate publication (manuscript in preparation).

pH Dependence of the Formation of the 430 nm Species in PR and D97N Mutant. The yield of the 430 nm species, negligible at neutral pH, increases manyfold with a pK_a of 2.6 upon decreasing the pH (Figure 4A), indicating that formation of the 9-*cis* photoproduct is strongly facilitated by the protonation of some acidic group(s). In an attempt to identify this residue, we examined the effects of neutralization of the two aspartates close to the chromophore, Asp97 and Asp227, on the pH dependence and the yield of 9-*cis* photoproducts (430 nm species).

At pH below 6, Asp97 is protonated in PR, so one would expect that at this pH range the D97N mutant would behave similarly to PR. This is indeed what was observed: light-induced formation of the 430 nm species in the D97N mutant was accompanied by a similar difference spectrum (Figure 4B) and exhibited pH dependence similar to that of PR, although with a pK_a increased somewhat, from 2.6 to 3.3 (Figure 4A). This result implies that Asp97 is not responsible for the manyfold increase of the yield of 9-*cis* species with pK_a around 3.

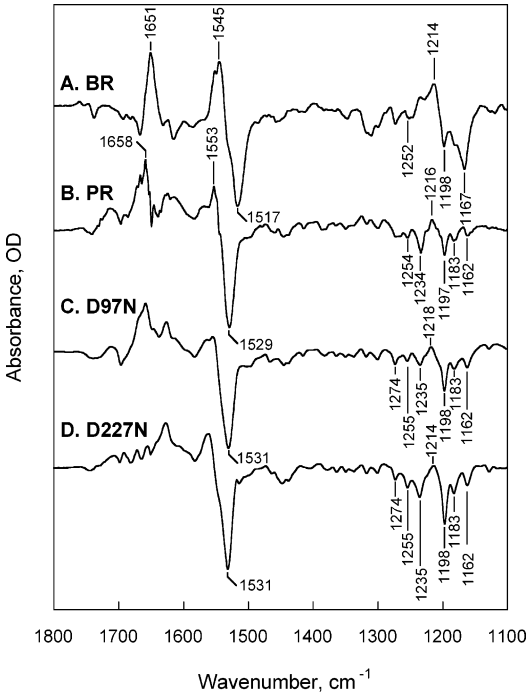

FIGURE 3: Light-induced FTIR difference spectra at acidic pH measured under >630 nm illumination for BR and under >530 nm for PR and its mutants. (A) BR at pH 2.3; (B) PR at pH 2.3; (C) D97N at pH 3.5; (D) D227N at pH 4. Purple membranes film was used for BR, while liposome-containing films were used for PR and its mutants. In BR the resulting pink membrane was quasi-stable (see also ref *18*), in PR the corresponding photoproducts partly relaxed back on the tens of minutes time scale. The spectra are scaled by the amplitude changes of their respective ethylenic bands, which were in the range of 0.02−0.04 OD.

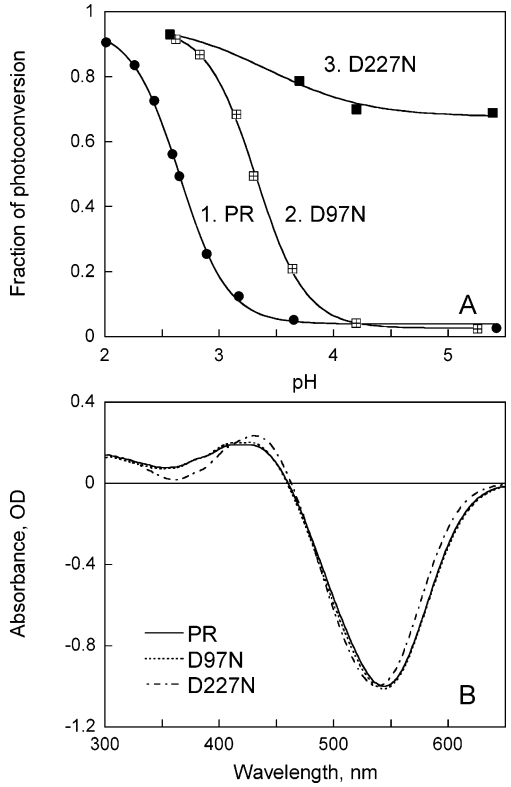

FIGURE 4: (A) pH dependence of the fraction of proteorhodopsin converted to the 430 nm species upon illumination for 5 min at λ > 530 nm: curve 1, PR; curve 2, D97N; curve 3, D227N. (B) Comparison of the light-induced difference spectra obtained upon illumination of PR, D97N, and D227N pigments. The spectrum for PR was measured at pH 2.5, and the others were at pH 3.

Dramatic Effect of the D227N Mutation on the Yield and pH Dependence of Light-Induced Conversion into 430 nm (9-cis) Species. The D227N mutation, on the other hand, results in facilitation of formation of the 430 nm species, which is observed in this mutant at a much higher pH than in PR and D97N (Figures 4 and 5). Illumination of the D227N pigment at pH 4 results in the formation of large amount of the 430 nm species (Figure 5A,B). Part of it can be reconverted back to the initial (or a spectrally similar) state (Figure 5B) by blue light. The 430 nm species is unstable in the dark. Within 30 min about 25% decays thermally back to initial pigment.

The strong pH dependence of the yield of the 430 nm species seen in PR and D97N mutant is less pronounced in D227N (Figure 4A). The pH dependence of the yield of 430 nm species reaches a plateau at pH between 4 and 6 in D227N indicating that neutralization of Asp227 by D227N mutation increases the yield of 9-*cis* species at this pH by at least 50-fold and largely eliminates its strong pH dependence. The yield of the 430 nm species exhibited linear dependence on light intensity (measured at pH 3). The quantum efficiency of formation of the long-lived 430 nm species in D227N is estimated to be about 0.01 at the pH range pH 4 to 5.

At pH above 6 illumination of D227N causes accumulation of a long-lived photoproduct with an absorption maximum at 365 nm. The yield of this species strongly increases with pK_a ca. 7.7. It has a decay time in tens of minutes (30 min at pH 8.2). In PR formation of a long-lived short wavelength photoproduct is observed also, but at a higher pH (above 9). The origin of these species will be a subject of a separate study.

DISCUSSION

We find that at low pH proteorhodopsin undergoes light-induced transformation to a long-lived species absorbing at 430 nm. FTIR measurements indicate that this species is 9-*cis*. Its yield is strongly pH dependent. In the pH range between 5 and 8 the yield is negligibly small but increases manyfold at acid pH, with a pK_a 2.6. The 430 nm species of proteorhodopsin is similar to the "pink membrane" formed by illumination of bacteriorhodopsin at low pH or after deionization (*18*−*20*). The D227N (but not the D97N) mutation increases the yield of 9-*cis* species at least 50-fold at pH 5, and to a large extent eliminates its pH dependency, indicating that it is the negatively charged Asp227 that prevents accumulation of 9-*cis* species in PR at pH > 3. Thus, Asp227 effectively controls the photoisomerization pathway so that isomerization around C_{13}═C_{14} bond is predominant in the functionally important pH range.

Mechanism of the Formation of the 9-cis Chromophore and pH Dependence of Its Yield. The observed isomerization from all-*trans* to 9-*cis* may, in principle, occur either as the primary photoreaction, or as a branching pathway, thermal or light-induced, upon absorption of a second photon by an intermediate of the photocycle. However, a branching pathway is very unlikely. Thermal conversion from 13-*cis* to 9-*cis* would require two C═C bond rotations, an event without precedence in retinal proteins. Further, isomerization

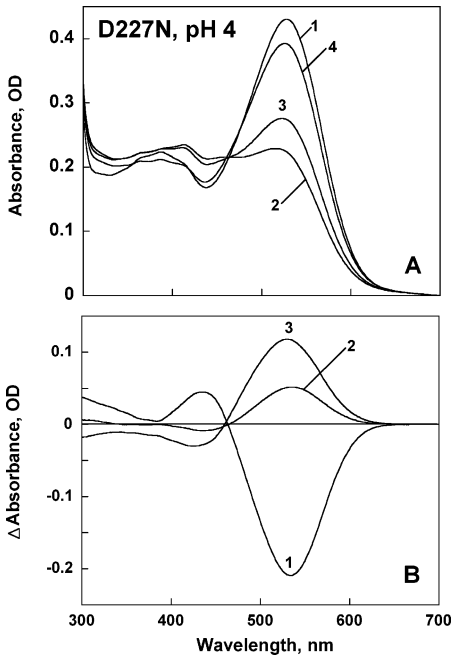

FIGURE 5: Absorption changes observed upon illumination of the D227N mutant at pH 4.0. (A) Absorption spectra: 1, initial D227N pigment at pH 4.0; 2, after illumination for 1 min at $\lambda > 530$ nm; 3, after 30 min in the dark; 4, after 2 min illumination at 407 nm. (B) Difference spectra: 1, produced by 1 min illumination at $\lambda > 530$ nm (curve 2 minus curve 1 on panel A); 2, absorption changes accompanying thermal conversion of the 430-nm photoproduct to initial pigment upon incubation in the dark for 30 min (curve 3 minus curve 2); 3, after subsequent 2 min illumination with blue light at 350−470 nm (curve 4 minus curve 3).

by a second quantum absorbed would result in quadratic light-intensity dependence for the initial rate of photoisomerization, and it was found to be linear. We conclude therefore that the isomerization to 9-*cis* is a primary photochemical event.

Photoisomerization of the all-*trans* retinal in the bacterial rhodopsins is normally restricted to the physiologically relevant 13-*cis*,15-*anti* configuration. The observation of a greatly enhanced production of the 9-*cis* species at low pH suggests that the charge environment of the retinal controls the course of the photoisomerization. The effect of the Asp227 mutation in PR that we report here strongly suggests that this negatively charged residue is a key factor in the constraints of the binding site imposed on the retinal chromophore so that all-*trans* → 13-*cis* isomerization is the main pathway under physiological conditions, and the alternative 9-*cis* isomerization, leading to a very slow photocycle (if any at all), is suppressed.

Comparison of the Photoconversions to 9-cis Products in Proteorhodopsin and Bacteriorhodopsin. Maeda et al. (*18*) found that continuous illumination of acid bacteriorhodopsin (called also blue membrane), which is a mixture of 40% 13-*cis*,15-*syn* and 60% *trans* and absorbs around 600 nm, with red light at pH 2 causing its transformation to species with maxima at 495 and 560 nm. The first of these states was the major product after long-term illumination, and was shown (through chromophore extraction and high-performance liquid chromatography) to contain 9-*cis* retinal, whereas the second had a 11-*cis* chromophore. Neither of these species was produced by illumination at neutral pH. The photoproducts could be reconverted back to the initial species (or a spectrally similar mixture of 13-*cis* and *trans* species) upon illumination with blue light. When the membranes containing the 495 nm photoproduct were brought to pH 9, the maximum shifted to 435 nm (perhaps due to Asp85 deprotonation). This species was also photosensitive and could be reconverted to BR. In the presence of hydroxylamine it slowly converted to retinal oxime in the dark, which absorbed at 360 nm. Interestingly, phototransformation to the 9-*cis* pigment was blocked in the "acid purple" species, which is formed at low pH in the presence of chloride.

Fischer et al. (*19*) obtained similar results regarding formation of 9-*cis* species, and in addition observed slow formation of a 390 species from a 450 nm species in the dark at pH 7. As the other 9-*cis* forms, it converted back to the initial BR upon illumination. The 390 nm species was a product of hydrolysis of the pigment. The authors pointed out that light-induced formation of 9-*cis* species originated from the initial BR (not from a photointermediate) since the yield depended linearly on light intensity.

Formation of the 9-*cis* species (pink membrane) was observed also from deionized (blue membranes) at pH 4.5 (*20*). The isomeric state of the chromophore was established by the chromatography (*20*) and resonance Raman spectroscopy (*21*). The quantum efficiency of transformation of the deionized (blue) membrane to the 9-*cis* photoproduct was estimated to be 1.6×10^{-4} at pH 5 and 0 °C (*26*). This is far below the quantum yield for photoisomerization to 13-*cis*, which is 0.6 (*27*, *28*). No pH dependence in the yield was observed in the pH range between pH 5 and 2.75. The efficiency of the reverse (pink → blue) photoreaction was 55-fold greater, 8.8×10^{-3}.

Illumination of some mutants of BR exhibited much increased yields of 9-*cis*, particularly the D212N mutant (*29*). Possible implication of Asp212 in photo (*29*−*31*) and thermal (*29*, *32*) isomerization was suggested earlier.

The photoconversions in PR can be summarized in the following way. Upon absorption of light all-*trans*-PR is converted to the excited-state PR*. At neutral pH most of the pigment undergoes all-*trans* → 13-*cis*,15-*anti* photoisomerization and proceeds through the photocycle which includes K, M, N (or O) (*5*, *6*, *33*), and within 100 ms returns to the initial state. However, there is a small probability of an alternative photoreaction which involves isomerization around $C_9{=}C_{10}$ double bond that leads to formation of 9-*cis* photoproducts, with absorption maximum at 430 nm.

The yield of the 9-*cis* species increases several orders of magnitude at low pH in PR and the D97N mutant, and in the D227N mutant occurs even at neutral pH. The latter indicates that neutralization of Asp227 leads to 9-*cis* photoproducts, whereas negatively charged Asp227 strongly favors all-*trans* → 13-*cis* isomerization.

If the reactions involving the 430 nm species can be regarded as a "9-*cis*" photocycle, it has a decay time of tens of mins and even longer, i.e., it is approximately 3 orders of magnitude slower than the 13-*cis* photocycle. The 9-*cis* cycle is likely to be a nonfunctional side-reaction of the pigment. However, it might be utilized as a sensory or regulatory reaction for detecting and avoiding high light intensity impacts. These reactions might be interesting also as a basis for photochromic applications, particularly since they yield long-lived photointerconvertible species.

The negative bands in the fingerprint region of the FTIR spectrum indicate that not only all-*trans* but also 13-*cis* isomers of initial PR convert to 9-*cis* species. The same conclusion can be drawn from the fact that most (>90%) of the pigment can be converted to 9-*cis* species under certain conditions. However, the results do not allow one to decide whether the conversion of 13-*cis* to 9-*cis* occurs directly or indirectly (through its thermal or light-induced conversion to all-*trans* and then to 9-*cis*). We favor the latter possibility.

Possible Mechanism of Involvement of Asp227 in Control of the Photoisomerization Pathway. An intriguing question is how the negatively charged Asp227 would prevent isomerization around the C_9=C_{10} double bond. One might consider two factors: electrostatic interaction of the carboxylate charge with the π-electron system of the chromophore and steric consequences of the neutralization of Asp227.

Earlier reports had suggested that in bacteriorhodopsin electrostatics strongly affects isomerization and related processes. A theoretical study (*34*) indicated that charges around the retinal might substantially affect the barriers for thermal isomerization. A model describing how the ionized carboxyls of Asp85 and Asp212 can affect the barriers and hence the rate constants for isomerization in the ground and excited state was proposed (*30*, *31*). It was shown that the rate of thermal all-*trans* ⇔ 13-*cis* isomerization (dark adaptation in BR) increases at low pH (*35*, *36*) and is proportional to the fraction of protonated Asp85 in BR (*37*−*39*). Neutralization of the latter results in at least 5000-fold increase in the rate of thermal isomerization (*37*, *39*) due to a decrease of the barrier for the isomerization presumably by an elimination of the electrostatic and hydrogen bonding interaction of the Schiff base and Asp85 (*39*, *40*).

The present study implies that in proteorhodopsin the negatively charged Asp227 interacts with the chromophore in such a way as to increase the barrier for rotation around the C_9=C_{10} bond in the excited state and decreases the barrier for the C_{13}=C_{14} isomerization. That would happen if the negative charge of Asp227 were closer to the C_{13}=C_{14} double bond than to any other. The structure for PR is not available but in BR the carboxyl of Asp212 is nearer to the C_{14} atom than any other part of the retinal, at 3.35 Å (*41*). Neutralization of the Asp227 negative charge by mutation or at low pH should eliminate this interaction, and elevate the barrier for rotation around the C_{13}=C_{14} bond. Correspondingly, isomerization elsewhere along the polyene chain, e.g., around the C_9=C_{10} double bond, might gain dominance.

One cannot exclude a second, alternative mechanism based on steric rearrangement of the chromophore binding site in response to protonation or neutralization of Asp227. The homologous residue in BR, Asp212, transiently protonates after the change of geometry at the active center upon thermal reisomerization of the retinal in the O photointermediate (*42*). In both cases (electrostatic and steric interactions) one would expect that the yield of 9-*cis* species at low pH would be proportional to the fraction of protonated Asp227. The titration-like strong pH dependence of the yield of 9-*cis* species at low pH in PR and D97N mutant (Figure 4A) is in agreement with this prediction.

An aspartic acid residue analogous to Asp227 of proteorhodopsin is strictly conserved among all retinal proteins with all-*trans* retinal as a chromophore. These include families of functionally diverse proteins in different kingdoms: archaeal proton pumps bacteriorhodopsin and archaerhodopsin, chloride pump halorhodopsin, sensory rhodopsins I and II (*43*, *44*), bacterial proteorhodopsins (*2*, *3*), *Neurospora* rhodopsin (*45*), sensory rhodopsin of *Chlamydomonas* (*46*). This implies that this aspartate is a principal element of light energy transduction in all these proteins. The data we obtained with proteorhodopsin and earlier data on bacteriorhodopsin (*29*−*31*) indicate that its function (or one of its functions) is to selectively catalyze the chromophore's all-*trans* → 13-*cis* photoisomerization, and possibly also the reverse thermal reisomerization, thus optimizing light energy conversion.

REFERENCES

1. Beja, O., Aravind, L., Koonin, E. V., Suzuki, M. T., Hadd, A., Nguyen, L. P., Jovanovich, S. B., Gates, C. M., Feldman, R. A., Spudich, J. L., Spudich, E. N., and DeLong, E. F. (2000) Bacterial rhodopsin: evidence for a new type of phototrophy in the sea. *Science 289*, 1902−1906.
2. Beja, O., Spudich, E. N., Spudich, J. L., Leclerc, M., and DeLong, E. F. (2001) Proteorhodopsin phototrophy in the ocean. *Nature 411*, 786−789.
3. Man, D., Wang, W., Sabehi, G., Aravind, L., Post, A. F., Massana, R., Spudich, E. N., Spudich, J. L., and Beja, O. (2003) Diversification and spectral tuning in marine proteorhodopsins. *EMBO J. 22*, 1725−1731.
4. Wang, W. W., Sineshchekov, O. A., Spudich, E. N., and Spudich, J. L. (2003) Spectroscopic and photochemical characterization of a deep ocean proteorhodopsin. *J. Biol. Chem. 278*, 33985−33991.
5. Dioumaev, A. K., Brown, L. S., Shih, J., Spudich, E. N., Spudich, J. L., and Lanyi, J. K. (2002) Proton transfers in the photochemical reaction cycle of proteorhodopsin. *Biochemistry 41*, 5348−5358.
6. Friedrich, T., Geibel, S., Kalmbach, R., Chizhov, I., Ataka, K., Heberle, J., Engelhard, M., and Bamberg, E. (2002) Proteorhodopsin is a light-driven proton pump with variable vectoriality. *J. Mol. Biol. 321*, 821−838.
7. Brown, L. S., Sasaki, J., Kandori, H., Maeda, A., Needleman, R., and Lanyi, J. K. (1995) Glutamic acid 204 is the terminal proton release group at the extracellular surface of bacteriorhodopsin. *J. Biol. Chem. 270*, 27122−27126.
8. Balashov, S. P., Imasheva, E. S., Ebrey, T. G., Chen, N., Menick, D. R., and Crouch, R. K. (1997) Glutamate-194 to cysteine mutation inhibits fast light-induced proton release in bacteriorhodopsin. *Biochemistry 36*, 8671−8676.
9. Dioumaev, A., Richter, H.-T., Brown, L. S., Tanio, M., Tuzi, S., Saito, H., Kimura, Y., Needleman, R., and Lanyi, J. K. (1998) Existence of a proton transfer chain in bacteriorhodopsin: Participation of Glu-194 in the release of protons to the extracellular surface. *Biochemistry 37*, 2496−2506.
10. Dioumaev, A. K., Wang, J. M., Balint, Z., Varo, G., and Lanyi, J. K. (2003) Proton transport by proteorhodopsin requires that the retinal Schiff base counterion Asp-97 be anionic. *Biochemistry 42*, 6582−6587.
11. Lakatos, M., Groma, G. I., Ganea, C., Lanyi, J. K., and Varo, G. (2002) Characterization of the azide-dependent bacteriorhodopsin-like photocycle of salinarum halorhodopsin. *Biophys. J. 82*, 1687−1695.
12. Varo, G., Brown, L. S., Lakatos, M., and Lanyi, J. K. (2003) Characterization of the photochemical reaction cycle of proteorhodopsin. *Biophys. J. 84*, 1202−1207.
13. Fischer, U., and Oesterhelt, D. (1979) Chromophore equilibria in bacteriorhodopsin. *Biophys. J. 28*, 211−230.
14. Mowery, P. C., Lozier, R. H., Chae, Q., Tseng, Y.-W., Taylor, M., and Stoeckenius, W. (1979) Effect of acid pH on the absorption spectra and photoreactions of bacteriorhodopsin. *Biochemistry 18*, 4100−4107.
15. Váró, G., and Lanyi, J. K. (1989) Photorections of bacteriorhodopsin at acid pH. *Biophys. J. 56*, 1143−1151.
16. Kelemen, L., Galajda, P., Száraz, S., and Ormos, P. (1999) Chloride ion binding to bacteriorhodopsin at low pH: an infrared spectroscopic study. *Biophys. J. 76*, 1951−1958.

17. Balashov, S. P., Govindjee, R., and Ebrey, T. G. (1991) Red shift of the purple membrane absorption band and the deprotonation of tyrosine residues at high pH. Origin of the parallel photocycles of *trans*-bacteriorhodopsin. *Biophys. J. 60*, 475−490.
18. Maeda, A., Iwasa, T., and Yoshizawa, T. (1980) Formation of 9-*cis* and 11-*cis*-retinal pigments from bacteriorhodopsin by irradiating purple membrane in acid. *Biochemistry 19*, 3825−3831.
19. Fischer, U., Towner, P., and Oesterhelt, D. (1981) Light indiced isomerization, at acidic pH, initiates hydrolysis of bacteriorhodopsin to bacterio-opsin and 9-*cis*-retinal. *Photochem. Photobiol. 33*, 529−537.
20. Chang, C.-H., Liu, S. Y., Jonas, R., and Govindjee, R. (1987) The pink membrane: the stable photoproduct of deionized purple membrane. *Biophys. J. 52*, 617−623.
21. Pande, C., Callender, R. H., Chang, C. H., and Ebrey, T. G. (1986) Resonance Raman study of the pink membrane photochemically prepared from the deionized blue membrane of *H. halobium*. *Biophys. J. 50*, 545−549.
22. Chang, C.-H., Jonas, R., Ebrey, T. G., Hong, M., and Eisenstein, L. (1987) Protonation changes in the interconversions of the pink membrane, blue membrane, and purple membrane in *Biophysical Studies of Retinal Proteins* (Ebrey, T. G., Frauenfelder, H., Honig, B., and Nakanishi, K., Eds.) pp 156−166, Department of Physics of the University of Illinois at Urbana-Champaign.
23. Smith, S. O., and Mathies, R. A. (1985) Resonance Raman spectra of the acidified and deionized forms of bacteriorhodopsin. *Biophys. J. 47*, 251−254.
24. Maeda, A. (1995) Application of FTIR spectroscopy to the structural study on the function of bacteriorhodopsin. *Isr. J. Chem. 35*, 387−400.
25. Smith, S. O., Lugtenburg, J., and Mathies, R. A. (1985) Determination of retinal chromophore structure in bacteriorhodopsin with resonance Raman spectroscopy. *J. Membr. Biol. 85*, 95−109.
26. Liu, S. Y., and Ebrey, T. G. (1987) The quantum efficiency for the interconversion of the blue and pink forms of purple membrane. *Photochem. Photobiol. 46*, 263−267.
27. Govindjee, R., Balashov, S. P., and Ebrey, T. G. (1990) Quantum efficiency of the photochemical cycle of bacteriorhodopsin. *Biophys. J. 58*, 597−608.
28. Tittor, J., and Oesterhelt, D. (1990) The quantum yield of bacteriorhodopsin. *FEBS Lett. 263*, 269−273.
29. Song, L., Yang, D., El-Sayed, M., and Lanyi, J. K. (1995) Retinal isomer composition in some bacteriorhodopsin mutants under light and dark adaptation conditions. *J. Phys. Chem. 99*, 10052−10055.
30. Song, L., El-Sayed, M. A., and Lanyi, J. K. (1993) Protein catalysis of the retinal subpicosecond photoisomerization in the primary process of bacterial photosynthesis. *Science 261*, 891−894.
31. Logunov, S. L., El-Sayed, M. A., and Lanyi, J. K. (1996) Catalysis of the retinal subpicosecond photoisomerization process in acid purple bacteriorhodopsin and some bacteriorhodopsin mutants by chloride ions. *Biophys. J. 71*, 1545−1553.
32. Seltzer, S. (1990) Models for bacteriorhodopsin-catalyzed dark *cis-trans* isomerization of bound retinal. *J. Am. Chem. Soc. 112*, 4477−4483.
33. Lakatos, M., Lanyi, J. K., Szakacs, J., and Varo, G. (2003) The photochemical reaction cycle of proteorhodopsin at low pH. *Biophys. J. 84*, 3252−3256.
34. Tavan, P., Schulten, K., and Oesterhelt, D. (1985) The effect of protonation and electrical interactions on the stereochemistry of retinal Schiff bases. *Biophys. J. 47*, 415−430.
35. Ohno, K., Takeyshi, Y., and Yoshida, M. (1977) Effect of light-adaptation on the photoreaction of bacteriorhodopsin from *Halobacterium halobium*. *Biochim. Biophys. Acta 462*, 575−582.
36. Warshel, A., and Ottolenghi, M. (1979) Kinetic and spectroscopic effects of protein-chromophore electrostatic interaction in bacteriorhodopsin. *Photochem. Photobiol. 30*, 291−293.
37. Balashov, S. P., Govindjee, R., Kono, M., Imasheva, E., Lukashev, E., Ebrey, T. G., Crouch, R. K., Menick, D. R., and Feng, Y. (1993) Effect of the arginine-82 to alanine mutation in bacteriorhodopsin on dark adaptation, proton release, and the photocheмical cycle. *Biochemistry 32*, 10331−10343.
38. Balashov, S. P., Govindjee, R., Imasheva, E. S., Misra, S., Ebrey, T. G., Feng, Y., Crouch, R. K., and Menick, D. R. (1995) The two pK_a's of aspartate-85 and control of thermal isomerization and proton release in the arginine-82 to lysine mutant of bacteriorhodopsin. *Biochemistry 34*, 8820−8834.
39. Balashov, S. P., Imasheva, E. S., Govindjee, R., and Ebrey, T. G. (1996) Titration of aspartate-85 in bacteriorhodopsin: What it says about chromophore isomerization and proton release. *Biophys. J. 70*, 473−481.
40. Logunov, I., and Schulten, K. (1996) Quantum chemistry: Molecular dynamics study of the dark-adaptation process in bacteriorhodopsin. *J. Am. Chem. Soc. 118*, 9727−9735.
41. Luecke, H., Schobert, B., Richter, H.-T., Cartailler, J.-P., and Lanyi, J. K. (1999) Structure of bacteriorhodopsin at 1.55 Å resolution. *J. Mol. Biol. 291*, 899−911.
42. Dioumaev, A. K., Brown, L. S., Needleman, R., and Lanyi, J. K. (1999) Fourier transform infrared spectra of a late intermediate of the bacteriorhodopsin photocycle suggest transient protonation of Asp-212. *Biochemistry 38*, 10070−10078.
43. Oesterhelt, D. (1998) The structure and mechanism of the family of retinal proteins from halophilic arhaea. *Curr. Opin. Cell Biol. 8*, 489−500.
44. Ihara, K., Umemura, T., Katagiri, I., Kitajima-Ihara, T., Sugiyama, Y., Kimura, Y., and Mukohata, Y. (1999) Evolution of the archaeal rhodopsins: evolution rate changes by gene duplication and functional differentiation. *J. Mol. Biol. 285*, 163−174.
45. Bieszke, J. A., Braun, E. L., Bean, L. E., Kang, S., Natvig, D. O., and Borkovich, K. A. (1999) The nop-1 gene of *Neurospora crassa* encodes a seven transmembrane helix retinal-binding protein homologous to archaeal rhodopsins. *Proc. Natl. Acad. Sci. U.S.A. 96*, 8034−8039.
46. Sineshchekov, O. A., Jung, K. H., and Spudich, J. L. (2002) Two rhodopsins mediate phototaxis to low- and high-intensity light in *Chlamydomonas reinhardtii*. *Proc. Natl. Acad. Sci. U.S.A. 99*, 8689−8694.

BI0355894